Pergamon

0301-9322(93)E0021-V

Int. J. Multiphase Flow Vol. 20, No. 3, pp. 481–491, 1994

0301-9322/94 $7.00 + 0.00

FRICTION FRACTOR AND HOLDUP STUDIES FOR LUBRICATED PIPELINING—II

LAMINAR AND k–ε MODELS OF ECCENTRIC CORE FLOW

A. HUANG,[1] C. CHRISTODOULOU[2] and D. D. JOSEPH[1]

[1]Department of Aerospace Engineering and Mechanics, University of Minnesota, 110 Union St S.E., 107 Akerman Hall, Minneapolis, MN 55455, U.S.A.

[2]Department of Mathematics, MIT, Cambridge, MA 02139, U.S.A.

(Received 18 July 1993; in revised form 17 November 1993)

Abstract—A model of core-annular flow in which the oil core is a perfect cylinder with generators parallel to the pipe wall, but off-center, is studied in laminar and turbulent flow to assess the effects of eccentricity and the volume flow rate ratio on the friction factor and holdup ratio. The study is tilted toward water lubrication of heavy crude viscous oil. For the turbulence analysis, the water is assumed to be turbulent and the core laminar. A standard k–ε model with a low Reynolds number capability is adopted for the turbulence case. The agreement between model predictions, which have no adjustable parameters, and experimental and field data from all sources, is satisfactory.

Key Words: core, annular, flow, lubricated, pipeline

1. INTRODUCTION

One method for transporting crude oil with substantial savings in power is by lubricating it with water. The water forms an annulus around a core of oil, reducing the shear stress on the wall of the pipe. Many studies of this topic, including a book (Joseph & Renardy 1993), have been published in recent years. For industrial design an applicable-Reynolds number–friction factor correlation is indispensable. Inspired by the Moody Chart for single-fluid pipeline systems, researchers have been trying to find a correlation between the Reynolds number and the friction factor for oil-in-water systems. Part I of this paper (Arney *et al.* 1993) presents one such study. Certain definitions of the friction factor and holdup ratio were shown to correlate the data from all lubricated pipelines with good agreements centered on rather large scatter. The scatter could be attributed to the eccentric position of heavier- or lighter-than-water oil cores, the effects of different holdup ratios, the increase in friction due to surface undulation and irregularities and to the fouling of pipe walls. In this part, we treat the same problem theoretically using the simplest models we could devise to assess the effects of eccentricity and turbulence without introducing fitting parameters. The model we use in both laminar and turbulent flow is perfect, off-center, core flow. The generators of the core and annulus are rigorously parallel and the cross section of the pipe and core is circular, but the centers do not coincide. This kind of model, for the laminar case, was introduced and studied by Bentwich (1964). He solved the Poisson equation [14] that governs in the eccentric core flow model with a Fourier series in bipolar coordinates. However, he did not use his solution to evaluate the friction factor or holdup.

Ooms *et al.* (1984) and Oliemans (1986) tried to use lubrication theory to analyze the case of a very viscous, wavy eccentric core and an annulus of water in laminar flow. By balancing the buoyancy with lubrication forces, they predicted the eccentricity of the core, and through numerical methods directly predicted the pressure drop. Their method works well for many, but not all, features of laminar flow when correct choices of the wave form and amplitude are assumed. Oliemans *et al.* (1987) also tried to extend their results to the turbulent case but again the theory requires the input of wave forms and wavelengths, which are harder to identify in the turbulent case. They used a mixing-length turbulent model with the Van Driest expression for the mixing length. Their turbulence model underpredicts the variation of the pressure gradient with oil

velocity, even when the actual wave amplitudes and wavelengths observed during their tests are used as input data. They speculated that their neglect of the Reynolds stress was the cause of the discrepancy.

In our analysis, we do not use fitting parameters such as the interfacial wave forms and we achieve good agreements, but we do not address the question of levitation of the core against gravity.

2. LAMINAR ECCENTRIC CORE FLOW

Consider a horizontal pipeline, within which two immiscible liquids flow in the axial direction. We refer to water as liquid 1 and oil as liquid 2, and assume that both liquids are Newtonian with different densities and viscosities. The constant diameter of the pipeline accomodates a uni-directional flow in the axial direction (x). A laminar core flow is a one-component velocity field $w(y, z)$ depending on the transverse coordinates y and z, satisfying the Navier–Stokes equations in reduced form:

$$-\rho g - \frac{\partial p}{\partial z} = 0 \qquad [1]$$

and

$$\mu \nabla^2 w - \frac{\partial p}{\partial x} = 0, \qquad [2]$$

where z increases against gravity. In [2], $\partial p/\partial x$ is the pressure gradient along x, which is a constant, f. On the pipe wall, the velocity must be zero,

$$w|_\Gamma = 0. \qquad [3]$$

We assume that the two liquids form only one interface Σ, i.e. cases for which there are more than one core of oil are excluded; Σ can be described as $\delta(z, y) = 0$. Across Σ the velocity and the shear stress are continuous:

$$[\![w]\!]|_\Sigma = 0 \qquad [4]$$

and

$$\left[\!\!\left[\mu \frac{\partial w}{\partial n}\right]\!\!\right]_\Sigma = 0, \qquad [5]$$

where $[\![\cdot]\!] = (\,)_1 - (\,)_2$ denotes the jump. The normal force balance on the interface involves

$$-[\![p]\!] + 2H\sigma = 0, \qquad [6]$$

where σ is the constant interfacial tension and $2H$, the mean curvature, is expressible as a differential form involving the function $\delta(x, y)$.

We can find the pressure from [1] and [2]:

$$p_i = -\rho_i \mathbf{g} z - \mathrm{f}x + \mathrm{C}_i \quad (i = 1, 2), \qquad [7]$$

where C_i are constants, one for each fluid. The pressure is determined up to an arbitrary constant which we choose to make $[\![\mathrm{C}]\!] = 0$. Then [6] and [7] imply that

$$[\![\rho]\!]\mathbf{g} \cdot \mathbf{x} + 2H\sigma = 0; \qquad [8]$$

integrating [8] over the circumference of the core, we have

$$[\![\rho]\!] \int_{\partial B} \mathbf{g} \cdot \mathbf{x} + 2\sigma \int_{\partial B} H = 0, \qquad [9]$$

where ∂B is the interface. Hesla *et al.* (1993) have shown that the term involving surface tension vanishes, hence

$$[\![\rho]\!] \int_{\partial B} \mathbf{g} \cdot \mathbf{x} = 0,$$

which is obviously false unless $[\![\rho]\!] = 0$. The mathematical contradiction we have just exposed is just a statement that if the density is not matched, the ideal core cannot be levitated against gravity.

The flow rates and the friction factor in a lubricated pipeline are of major concern in applications. The volume rate is defined as

$$Q_i = \int_{\Omega_i} w_i \, d\Omega, \qquad [10]$$

where Ω_i is the area occupied by fluid i. From Q_1 and Q_2 a volume average velocity is defined:

$$V = \frac{Q_1 + Q_2}{\pi R^2}, \qquad [11]$$

where R is the radius of the pipe. The friction factor is a measure of the shear stress on the wall, it is defined (Arney *et al.* 1993) as:

$$\lambda = \frac{8\tau_w}{\rho V^2}; \qquad [12]$$

τ_w is the shear stress, which is related to the constant pressure gradient f along the axial direction by

$$\tau_w = \frac{R\mathrm{f}}{2}.$$

Then,

$$\lambda = \frac{4R\mathrm{f}}{\rho V^2}.$$

Using [11], we get

$$\lambda = \frac{\mu_1}{2R\rho V} \frac{8\pi R^4 \mathrm{f}}{\mu_1 (Q_1 + Q_2)} = \frac{\beta}{\mathrm{Re}},$$

with Re as a Reynolds number and

$$\beta = \frac{8\pi R^4 \mathrm{f}}{\mu_1 (Q_1 + Q_2)}. \qquad [13]$$

In experiments and industrial applications the holdup fraction H_w and the input fraction C_w of water are the two most used parameters. They are defined (Arney *et al.* 1993) as:

$$H_w = \frac{\mathscr{V}_1}{\mathscr{V}_1 + \mathscr{V}_2}$$

and

$$C_w = \frac{Q_1}{Q_1 + Q_2},$$

where $\mathscr{V}_1$ is the volume of water and $\mathscr{V}_2$ is the volume of oil. In our case, because the flow field is two-dimensional, $\mathscr{V}_1$ and $\mathscr{V}_2$ are just the areas occupied by the fluids on the cross section and C_w can be regarded as the flux ratio of water.

Introducing dimensional scales for length and velocity, respectively, as R and $\mathrm{f}R^2/\mu_1$, we make the equations dimensionless:

$$\left.\begin{aligned} \nabla^2 w_1 &= 1, \quad \text{in } \Omega_1 \\ \nabla^2 w_2 &= m, \quad \text{in } \Omega_2 \\ w_i &= 0, \quad \text{on } \Gamma \backslash \Sigma \end{aligned}\right\} \qquad [14]$$

and

$$[\![w]\!] = \left[\!\left[m \frac{dw}{dn} \right]\!\right] = 0, \quad \text{on } \Gamma/\Sigma,$$

where $m(<1)$ is the viscosity ratio μ_1/μ_2 and w is the dimensionless velocity.

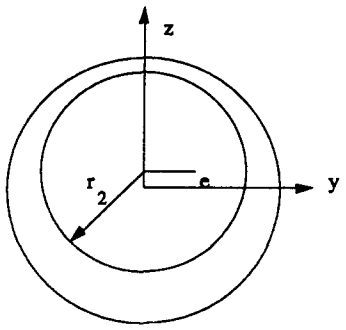

Figure 1. Eccentric core flow. All lengths are dimensionless in units of r, the radius of the pipe. The coordinate z is against gravity. The core and pipe have circular cross sections with parallel axes along x (not shown) through centers which are a distance e apart.

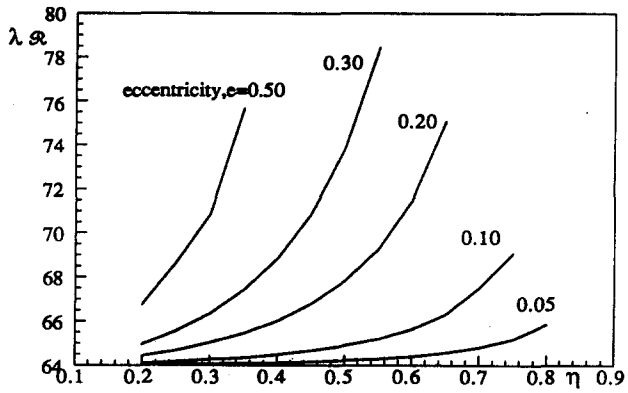

Figure 2. The product $\lambda\Re$ of the friction factor and Reynolds number vs η for $m = 1/90{,}000$ and different eccentricities e, in the laminar case. The friction factor is greater for larger eccentricity.

When $[\![\rho]\!] = 0$, gravity does not enter into the dynamics and the cross section of the core reduces to a circle. However, the radius r_2 and the position of the core, which can be represented by the eccentricity e as shown in figure 1, must be prescribed so that the interface can be specified completely.

From [12] it can be easily seen that β is only a function of e, m and $\eta(=r_2)$, the radius ratio, after we introduce the dimensionless quantities into the formulas. So

$$\lambda = \frac{\beta(e, m, \eta)}{\mathrm{Re}}.$$

$e = 0$ is the concentric case, which has been the subject of many theoretical studies (Joseph & Renardy 1993) and the results of the studies have been widely compared with experiments. In this case, the system can be solved explicitly. In dimensionless form, we have

$$w_1 = (1 - r^2) \quad \text{and} \quad w_2 = m(\eta^2 - r^2) - \eta^2 + 1,$$

where r is the radius of cylindrical coordinates. The flow rates Q_1 and Q_2 are then obtained easily and

$$\beta(0, m, \eta) = \frac{64}{1 + \eta^4(m - 1)}.$$

If we redefine the Reynolds number as [see Arney *et al.* (1993) for a discussion of $\Re$]:

$$\Re = \frac{\mu_1}{2R\rho V}[1 + \eta^4(m - 1)] = \mathrm{Re}[1 + \eta^4(m - 1)], \qquad [15]$$

we have

$$\lambda = \frac{64}{\Re}.$$

In general case $e \neq 0$, the problem is solved numerically by a finite element method. The product of the friction factor and Reynolds number, $\lambda\Re$, in these eccentric cases is shown in figure 2, where $\lambda\Re$ is plotted as a function of e and η for a fixed viscosity ratio $m = 1/90{,}000$, which is common for heavy crude oil and water. It is clear from the results that $\lambda\Re > 64$ when $e \neq 0$; physically, this means that the friction on the wall is larger under the same Reynolds number when the core is off-center, although the friction is not greatly different than when $e = 0$. For a fixed e, the friction increases with increasing core radius.

Using the same parameters, the results of holdup fraction H_w vs the volume flow rate of water C_w are plotted in figure 3. The results when the core is off-center do not differ much from the concentric case (Arney *et al.* 1993) even for $e = 0.5$.

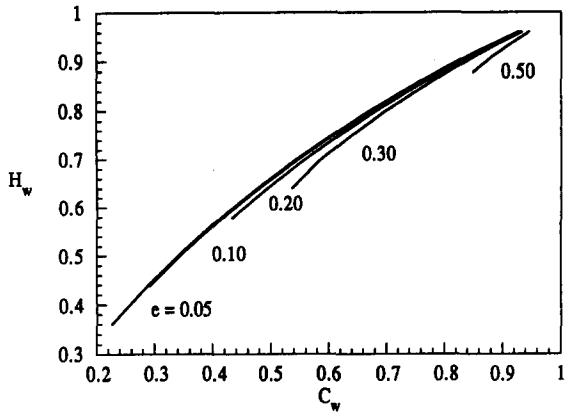

Figure 3. The water holdup H_w vs the volume flow rate C_w for the same parameters as in figure 2 and different values of the eccentricity e. The holdup is not a sensitive function of the eccentricity in laminar flow (or turbulent flow, see figure 12).

3. TURBULENT ECCENTRIC CORE FLOW

Because the viscosity of the oil is large, we may assume that the flow is laminar in the oil core, while turbulent in the water annulus. Overall the flow is fully developed with one non-zero component of the mean velocity. To compute the turbulent flow in the water we used the k–ε model.

In order to cover the range of Reynolds numbers encountered in practice, a so-called low Reynolds number k–ε model was chosen. This model is not restricted to high Reynolds numbers for which certain wall functions are required, but rather extends the range of validity of the model to lower Reynolds numbers (Launder & Spalding 1974).

3.1. The k–ε equations

Let k and ε be the turbulent energy and the dissipation rate of this energy, respectively. Launder & Spalding (1974) proposed a set of equations for k and ε, for our steady two-dimensional case they are the following:

$$\mathrm{div}\left[\left(\frac{\mu_t}{\sigma_k}+\mu\right)\nabla k\right]+\mu_t\left[\left(\frac{\partial w}{\partial r}\right)^2+\left(\frac{1}{r}\frac{\partial w}{\partial \theta}\right)^2\right]-2\mu\left[\left(\frac{\partial k^{1/2}}{\partial r}\right)^2+\left(\frac{1}{r}\frac{\partial k^{1/2}}{\partial \theta}\right)^2\right]-\rho\varepsilon=0 \quad [16]$$

and

$$\mathrm{div}\left[\left(\frac{\mu_t}{\sigma_\varepsilon}+\mu\right)\nabla\varepsilon\right]+C_1\frac{\varepsilon}{k}\frac{\mu_t}{r}\left[\left(\frac{\partial w}{\partial r}\right)^2+\left(\frac{1}{r}\frac{\partial w}{\partial \theta}\right)^2\right]+2\upsilon\mu_t\left[\left(\frac{\partial^2 w}{\partial r^2}\right)^2+\left(\frac{1}{r^2}\frac{\partial^2 w}{\partial \theta^2}\right)^2+2\left(\frac{1}{r}\frac{\partial^2 w}{\partial\theta\partial r}\right)^2\right]-C_{2\varepsilon}\rho\frac{\varepsilon^2}{k}=0, \quad [17]$$

where w is the axial direction component of the mean velocity, satisfying

$$\mathrm{div}[(\mu_t+\mu)\nabla w]-\frac{\partial p}{\partial x}=0 \quad [18]$$

where μ_t is the eddy viscosity, modeled as

$$\mu_t=C_\mu\frac{k^2}{\varepsilon}. \quad [19]$$

In the above equations, C_1, σ_k and σ_ε are constants, whose values were determined by fitting computations to experiments. The commonly accepted values of these constants are

$$C_1=1.44, \quad \sigma_k=1.0 \quad \text{and} \quad \sigma_\varepsilon=1.3.$$

C_μ and $C_{2\varepsilon}$ vary with the turbulent Reynolds number,

$$R_t=\frac{k^2}{\nu\varepsilon}, \quad [20]$$

according to the formulas

$$C_\mu = C_{\mu\infty} \exp\left(-\frac{2.5}{1 + \frac{R_t}{50}} \right)$$

and

$$C_{2\varepsilon} = C_{2\infty}[1.0 - 0.3 \exp(-R_t^2)],$$

where $C_{2\infty} = 1.92$ and $C_{\mu\infty} = 0.09$ are the constants used for fully developed turbulence.

Launder & Spalding (1974) introduced the extra term

$$-2\mu\left[\left(\frac{\partial k^{1/2}}{\partial r}\right)^2 + \left(\frac{1}{r}\frac{\partial k^{1/2}}{\partial \theta}\right)^2\right]$$

in the k equation in order to implement a zero boundary condition for ε. Although ε goes to a constant on the wall, this treatment of the boundary condition seemed to work better than using the zero-gradient boundary condition for ε. Our work confirmed this.

Other boundary conditions include the zero conditions for k and w on the pipe wall. In the interior of the oil core we simply require that k, ε and the eddy viscosity μ_t be zero because of the laminar flow assumption. This also ensures the continuity of the mean velocity and mean shear stress across the interface between the oil core and the water annulus.

We use a Patankar–Spalding code to solve the k–ε problem. This control-volume code is quite general and works well for convection–diffusion type equation in two-dimensional domains, including k–ε model equations (Jones & Launder 1972; Launder & Spalding 1974).

3.2. Validity of the numerical simulation

The eccentricity of the core is produced by the dynamics of levitation neglected here. The position of the core in our model has to be given as an input. The concentric case is the simplest because it leads to ordinary differential equations depending on the radius r alone.

Turbulence models should be validated by comparing measured and predicted values of the velocity profile. The only measured velocity profile known to us was by Sinclair (1970). Since his results were not for perfect core-annular flow, we are not able to make a direct comparison. Nevertheless, comparisons of this type for single-fluid flow in a pipe (Launder & Spalding 1974) have shown good agreements. In the development of the so-called Reynolds number model, special attention was given to matching the velocity profile close to the wall, the so-called logarithmic region, since that is where the model differs from the regular k–ε model. Although our case is different, we expect that the velocity profile close to the wall and the interface should resemble those of a single-fluid flow in a pipe. In figure 4 the velocity profile close to the wall is plotted in wall units, i.e.

$$y^+ = \frac{u_\tau (R - r)}{\nu}$$

where

$$u_\tau = \left(\frac{\tau_w}{\rho}\right)^{1/2}$$

is the friction velocity, τ_w is the shear stress on the wall and $u^+ = w/u_\tau$. Figure 5 shows a similar plot near the interface. These figures show that our computed profiles are similar to the profiles given in the literature (Launder & Spalding, figure 3.3) for turbulent shear flows. Figure 6 shows graphs of the turbulent kinetic energy k and the turbulent energy dissipation rate ε in wall units

$$k^+ = \frac{k}{u_\tau^2} \quad \text{and} \quad \varepsilon^+ = \frac{\nu\varepsilon}{u_\tau^4};$$

k and ε have shapes that are typical of a turbulent shear flow of a single fluid (Patel *et al.* 1984, see figure 1). This comparison serves as another justification for our numerical computation.

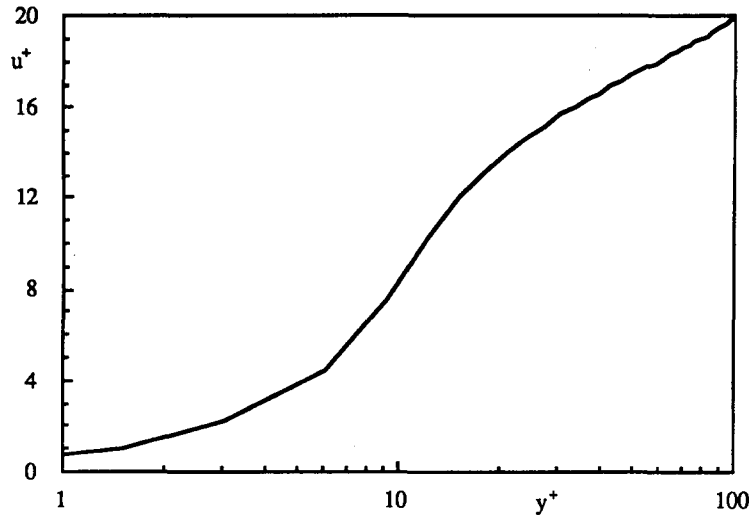

Figure 4. Computed turbulent mean velocity profile near the wall: $\Re = 21{,}000$, $m = 1/2000$, $\eta = 0.8$ and $e = 0.0$.

3.3. Turbulent exponent for the friction factor

Figures 7 and 8 are the computed velocity profiles for concentric core flow with a viscosity ratio of 1/2000 when the radius of the core is 80% of that of the pipe. The velocity in figure 7 is expressed in units of fR^2/μ_w and has been plotted for different Reynolds numbers.

The oil core moves like a rigid body because it is so viscous. However, the forward speed of the core is to be determined by the retarding shear in the water. We may collapse the profiles in figure 7 by rescaling the velocity with $\Re^{-0.79}$. The result is shown in figure 8. It is clear that the newly-scaled velocity profiles for different Reynolds number do not differ much. We shall see later that the holdup ratio does not depend strongly upon the Reynolds number because the velocity profiles are more or less self similar. However, in general, it is not always possible to get such a good collapse with a single factor of $\Re$. Finally, we note that a Blausius formula for turbulence states that the velocity profile scales as $\Re^{-0.75}$; the power index from our computation depends on the radius ratio η and is around 0.79. This suggests that other classical properties of turbulence in pipe flow might also find an appreciation in the study of turbulent two-phase core flow. For example, roughness correlations could be used to describe the rise of the friction factor observed in fouled lines.

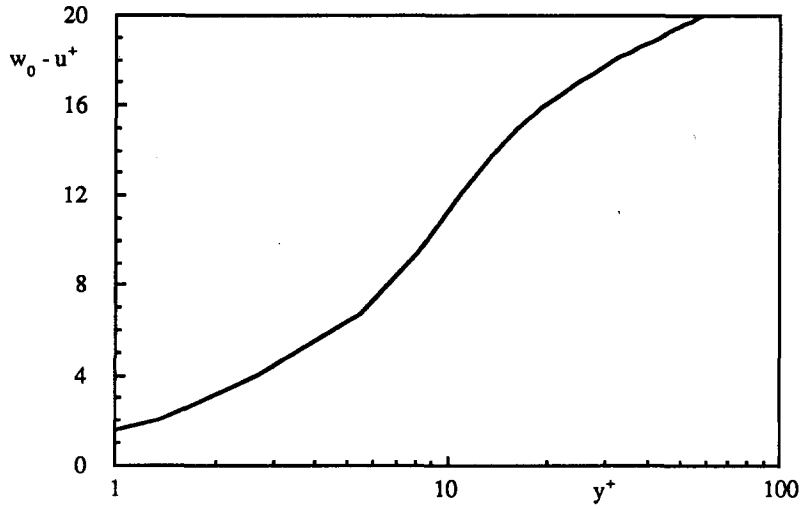

Figure 5. Computed turbulent mean velocity profile near the interface for the same parameters as in figure 4; w_0 is the forward speed of the interface.

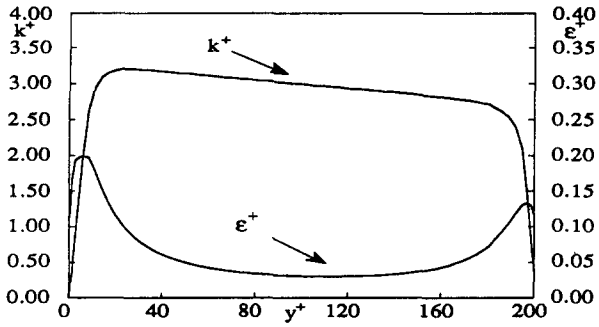

Figure 6. Turbulent kinetic energy and the dissipation rate of this energy in universal turbulent coordinates; $\Re = 21{,}000$, $m = 1/2000$, $\eta = 0.8$ and $e = 0.0$

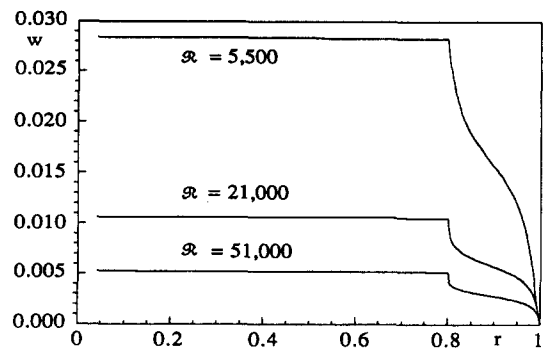

Figure 7. Turbulent mean velocity profiles for different Reynolds numbers; $m = 1/2000$, $\eta = 0.8$ and $e = 0.0$

When the velocity profile is known, the friction factor λ can be readily computed. For a given pressure gradient, a velocity profile is computed. Then we calculate the average velocity V. Using V, we compute a Reynolds number [15] and λ. This procedure gives a point in the friction factor–Reynolds number plane. Figure 9 gives such a plot for concentric flow, where the different symbols represent data from different sources [see Arney *et al.* (1993) for more details]. The friction factor for laminar flow is also displayed in figure 9 as the straight line $\lambda = 64/\Re$. In general, our computational results agree well with the experimental data given by Arney *et al.* (1993). Larger values of the radius ratio η lead to lower values of λ. This is because the oil moves as a rigid body with a velocity higher than that of the water so that the average velocity increases with η, which in turn gives a lower value of λ. This is also one of the reasons that data from the experiments scatters.

3.4. Effect of the viscosity ratio

We have assumed that the flow in the interior of the oil core is laminar. This is based upon the assumption that the viscosity of the oil is much larger than that of the water. In the concentric case we calculated the friction factor for different values of the viscosity ratio m with the results shown in figure 10. A hugh increase in m leads to only a slightly smaller friction factor. As long as the viscosity ratio is small enough, say $< 1/1000$, any decrease in m will have virtually no effect on the friction factor.

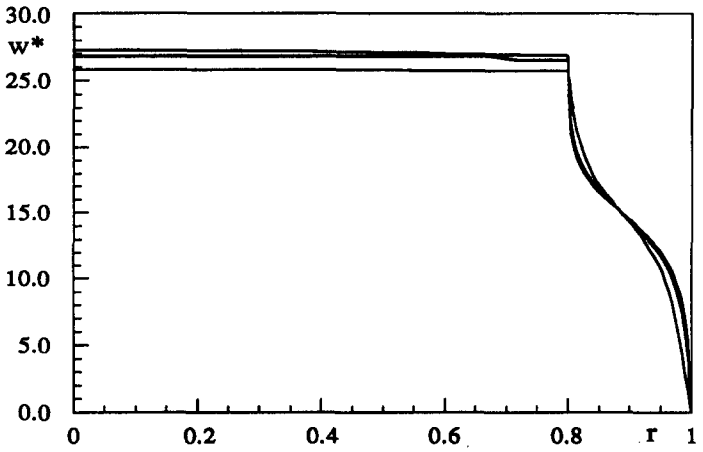

Figure 8. The same velocity profiles as in figure 7 but rescaled by $\Re^{-0.79}$, i.e. $w^* = w\Re^{0.79}$. The turbulence exponent 0.79 for core flow can be compared with the Blausuis exponent of 0.75 for pipe flow of a single fluid.

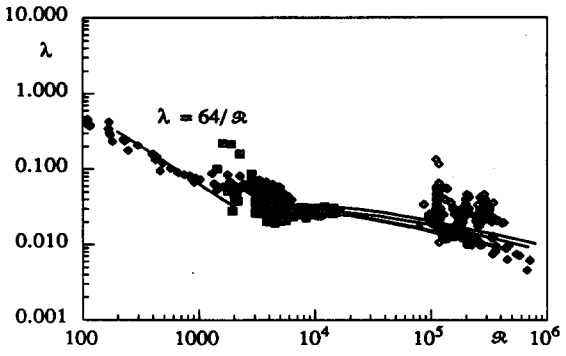

Figure 9. Friction factor vs Reynolds number in the concentric case ($e = 0.0$) for $m = 1/2000$ and $\eta = 0.7$, 0.8 and 0.9. The smallest λ, the line at the bottom, corresponds to the largest η; i.e. the smallest water fraction. More water increases the friction factor slightly. The data is from Arney *et al.* (1993).

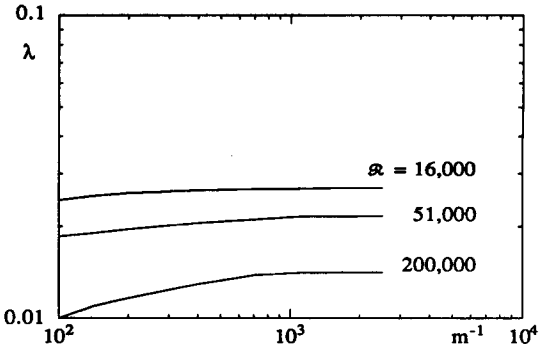

Figure 10. Friction factor vs viscosity ratio for different Reynolds numbers when $\eta = 0.8$. The friction factor is insensitive to the viscosity ratio for sufficiently small m.

3.5. Effect of eccentricity

It is evident that a perfect concentric flow is a very rare event, possible only in the smallest window of parameters. Even when the flow is laminar, the instability from the interfacial friction produces waves on the core (Joseph & Renardy 1993). Moreover, since the densities of the two fluids are almost always different, gravity will push the core off-center. Experimental results suggest that under normal conditions an eccentric core-annular flow, rather than a stratified flow, is achieved. In this case the eccentric core cannot be a perfect cylinder. A wavy interface is needed to levitate the core. Apart from proposals (Ooms *et al.* 1984; Oliemans 1986; Oliemans *et al.* 1987) based on lubrication theory, an explanation of the mechanism has yet to be established. We know that there must be a secondary flow in the pipe and the eccentricity must be related to the density difference, however there are no experimental results to guide us on this matter. For our computation, we simply input the eccentricity, assuming that we have a perfect eccentric core-annular flow, and compute the friction factor. Results of these computations are shown in figure 11; the viscosity ratio is 1/2000, $\eta = 0.7$, three different values of $e(= 0.0, 0.10, 0.15)$ are plotted and, as a comparison, the corresponding laminar case is also displayed as straight lines to the left. In general, an eccentric flow gives a higher value of the friction factor, although the difference is not large except at a very high Reynolds number.

We also computed holdups under the conditions specified in figure 11, with the results shown in figure 12. This shows that the k–ε model gives rise to holdup ratios, which like the experiments

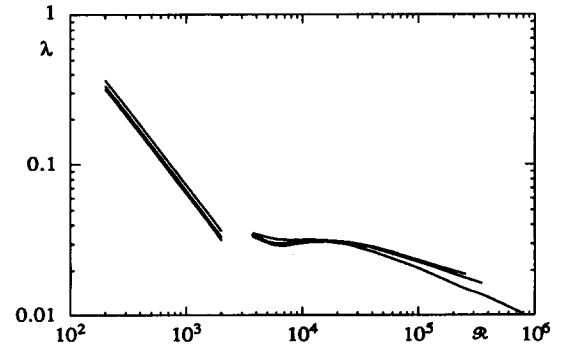

Figure 11. Friction factor vs Reynolds number for $\eta = 0.7$, $m = 1/2000$ and different eccentricities, $e = 0.00$, 0.10 and 0.15. The larger the eccentricity, the larger the friction factor.

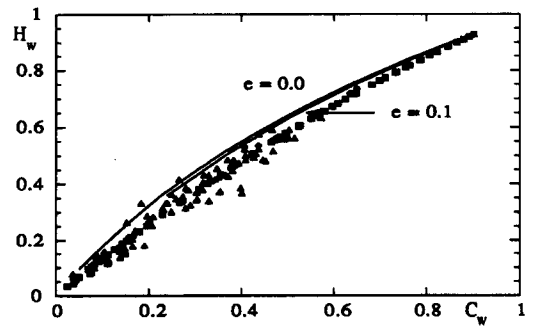

Figure 12. The water holdup H_w vs the volume flow rate C_w for turbulent flow; $m = 1/2000$ and $\Re = 21{,}000$. The experimental data is from Arney *et al.* (1993).

reviewed in part I (Arney *et al.* 1993), do not depend strongly on the Reynolds number. For Reynolds number from 5000 to 250,000, the variation in C_w for a fixed value of H_w is $< 5\%$. As we mentioned earlier, this independence is associated with the fact that the shapes of the velocity profile are nearly independent of $\Re$. We note that, in general, the computational results give lower values of C_w than are found in experiments. This is because we have not taken into account the roughness of the surface of the core, which will certainly allow more oil to flow through, giving a lower flux ratio of the water. An eccentric core results in a higher value of C_w and brings the computed curve into better agreement with the experimental data.

4. CONCLUSIONS

A model of core-annular flow in which the oil core is a perfect cylinder with generators parallel to the pipe wall, but off-center, was studied in laminar and turbulent flow to assess the effects of eccentricity and the volume flow rate on the friction factor and water holdup. In our model the oil is not allowed to touch the pipe wall. If the density of the oil and water are different, a perfect core cannot be levitated against gravity. A lift mechanism which decides where the levitated core is located must be associated with surface irregularities, but is neglected here. In the model, the eccentricity is prescribed. The problem of perfect eccentric laminar core flow was solved by a finite element method. The friction factor for laminar flow with different eccentricities is slightly above the line $64/\Re$ for concentric flow. The greater the eccentricity, the greater the discrepancy. This kind of behavior is in good agreement with the experiments (figure 9) which show data clustered around the pencil of lines near $64/\Re$. Some of the data in the laminar region lie further above this pencil of lines. The cause of this discrepancy is not known but may presumably be associated with the fact that many laminar flows are for other than perfect eccentric core flow; e.g. slugs, bubbles and large amplitude waves are observed. The water holdup is rather insensitive to changes in eccentricity (figures 3 and 12).

For the turbulence analysis, the water is assumed to be turbulent and the core laminar. The same geometric model and a standard k–ε model with a low Reynolds number capability (Launder & Spalding 1974) is adopted for the turbulence model. The model was solved with the control volume code SIMPLER.

The agreement between the computed friction factors that form the pencil of curved lines for large $\Re$ and the experimental data is excellent (figure 9). The power index for our computation is around 0.79, rather than the Blausius value of 0.75, and this value varies slightly with the ratio η. The computed results and the data do not change much with the viscosity ratio for small ratios (figure 10). Friction factors are increasingly higher with a higher water fraction for concentric flow; or with higher eccentrictiy for the eccentric case. A property that appears to be shared by the data (figure 9) at lower $\Re$ is that the friction factor decreases through a local mimimum, rises to a local maximum and then decreases monotonically (figure 11). At high Reynolds number, figure 9 shows some data that fall rather far above the computed correlation. Arney *et al.* (1993) attributed this discrepancy to oil fouling the pipe walls, it is possible that the degree of fouling could be described by the roughness correlation as in the empirical theory of turbulent pipe flow of one fluid [for instance, see Schlichting (1960, figure 20.18)].

The water holdup is almost a unique function of the flow rate ratio with little deviation for different eccentricities near to zero (figure 12). The data shares this property.

It is of considerable interest that we get good agreements without fitting parameters or looking very closely at waves or irregularities of the core.

As a final remark, we note that the k–ε model we used and other k–ε models do not give rise to unique solutions, in addition to the computed one, $k = \varepsilon = \mu_t = 0$ everywhere is also a solution, and other unphysical solutions in which k and ε change sign may also exist.

Acknowledgements—This work was supported by grants from the ARO (Mathematics), AHPCRC, the National Science Foundation and the Minnesota Supercomputer Center. The authors wish to thank Professor S. Patankar (Department of Mechanical Engineering, University of Minnesota) for providing us with the computer code and very sound advice.

REFERENCES

ARNEY, M. S., BAI, R., GUEVARA, E., JOSEPH, D. D. & LIU, K. 1993 Friction factor and holdup studies for lubricated pipelining—I. Experiments and correlations. *Int. J. Multiphase Flow* **19,** 1061–1076.

BENTWICH, M. 1964 Two-phase viscous axial flow in a pipe. *J. Bas. Engng* 669–672.

HESLA, T., HUANG, A. & JOSEPH, D. D. 1993 A note on the net force and moment on a drop due to surface forces. *J. Colloid Interface Sci.* **158,** 255–257.

JONES, W. P. & LAUNDER, B. E. 1972 The prediction of laminarization with a two-equation model of turbulence. *Int. J. Heat Mass Transfer* **15,** 301–314.

JOSEPH, D. D. & RENARDY, Y. 1993 *Fundamentals of Two-fluid Dynamics*, Part II. Springer-Verlag, New York.

LAUNDER, B. E. & SPALDING D. B. 1974 The numerical computation of turbulence flows. *Comput. Meth. Appl. Mech. Engng* **3,** 269–289.

OLIEMANS, R. V. A. 1986 *The Lubricating Film Model for Core-annular Flow*. Ph.D. Thesis, Delft Univ. Press, Technische Hogeschool Delft, The Netherlands.

OLIEMANS, R. V. A., OOMS, G., WU, H. L. & DUIJVESTIJN, A. 1987 Core-annular oil/water flow: the turbulent-lubricating-film model and measurements in a 5 cm pipe loop. *Int. J. Multiphase Flow* **13,** 22–31.

OOMS, G., SEGAL, A., VAN DER WEES, A. J., MEERHOFF, R. & OLIEMANS, R. V. A. 1984 The theoretical model for core-annular flow of a very viscous oil core and a water annulus through a horizontal pipe. *Int. J. Multiphase Flow* **10,** 41–40.

PATEL, V. C., ROOI, W. & SCHEUERER, G. 1984 Turbulence models for near-wall and low Reynolds number flows: a review. *AIAA Jl* **23.**

SCHLICHTING, H. 1960 *Boundary Layer Theory*. Pergamon Press, New York.

SINCLAIR, A. R. 1970 Rheology of viscous fracturing fluids. *J. Pet. Technol.* **June,** 711–719.